
UNIVERSAL SCALE-FREE REPRESENTATIONS IN HUMAN VISUAL CORTEX

A PREPRINT

Raj Magesh Gauthaman¹ , Brice Ménard^{2,1,3} , Michael F. Bonner¹ 

¹Department of Cognitive Science, ²Department of Physics and Astronomy

Johns Hopkins University, Baltimore, MD

³Santa Fe Institute, Santa Fe, NM

{rgautha1, menard, mfbonner}@jh.edu

ABSTRACT

How does the human visual cortex encode sensory information? To address this question, we explore the covariance structure of neural representations. We perform a cross-decomposition analysis of fMRI responses to natural images in multiple individuals from the Natural Scenes Dataset and find that neural representations systematically exhibit a power-law covariance spectrum over four orders of magnitude in ranks. This scale-free structure is found in multiple regions along the visual hierarchy, pointing to the existence of a generic encoding strategy in visual cortex. We also show that, up to a rotation, a large ensemble of principal axes of these population codes are shared across subjects, showing the existence of a universal high-dimensional representation. This suggests a high level of convergence in how the human brain learns to represent natural scenes despite individual differences in neuroanatomy and experience. We further demonstrate that a spectral approach is critical for characterizing population codes in their full extent, and in doing so, we reveal a vast space of uncharted dimensions that have been out of reach for conventional variance-weighted methods. A global view of neural representations thus requires embracing their high-dimensional nature and understanding them statistically rather than through visual or semantic interpretation of individual dimensions.

1 Introduction

How does the human visual cortex leverage the activity of large-scale neural populations to represent sensory information? To what extent are these visual population codes shared across individuals? Shedding light on these questions can be done by studying the covariance structure of neural populations, a quantity describing important aspects of information processing in neural population activity.

While previous studies have examined the covariance of visual cortex activity in humans and monkeys, they have largely done so in the service of dimensionality reduction (Haxby et al., 2011; Huth et al., 2012; Khosla et al., 2022; Tarhan & Konkle, 2020). Some of these studies have argued that dimensionality reduction is implemented by visual cortex itself to achieve stable representations of behaviorally relevant information (Fusi et al., 2016; Lehky & Tanaka, 2016; Lehky et al., 2014). Others have used dimensionality reduction as a tool to uncover individual representational dimensions that can be semantically interpreted (Connolly et al., 2012; Huth et al., 2012; Khosla et al., 2022; Thorat et al., 2019). Together, these studies have provided valuable insight into the leading and highest-variance dimensions of visual cortex activity, but none have attempted to provide a global characterization of how cortical populations encode sensory information. To understand the sensory code in its entirety, we need to go beyond its leading dimensions and examine stimulus representations at all levels of variance: we need to characterize its spectrum as broadly as possible.

It is also crucial to understand which aspects of visual cortex representation are shared across individuals and thus reflect general properties of human vision. A number of studies have addressed this question using representational similarity analysis (RSA) and hyperalignment (Haxby et al., 2011, 2020; Kriegeskorte, 2008). However, these previous studies have not examined the *extent* to which the underlying dimensions of the cortical sensory code are shared across individuals. Thus, several fundamental questions remain unanswered. Over how many dimensions is the shared representation expressed? Do subjects represent images similarly across all ranks of latent dimensions, or is the shared code restricted to a core subset of dimensions?

Here we explore the structure of visual neural representations following a methodological approach closer to physics than traditional neuroscience. We characterize, as broadly as possible, the spectrum of representational dimensions that co-vary between trials or subjects. We do so by leveraging a large-scale dataset of high-resolution fMRI responses to thousands of natural images (Allen et al., 2021). Using an orthogonal cross-decomposition with a generalization test on held-out images, we show that the covariance spectrum of fMRI responses to natural images in human visual cortex is consistent with a power-law distribution over almost four orders of magnitude in latent dimension ranks. This reveals that the statistics of neural activations are *scale-free*, a behavior we observe across all individuals and in multiple visual regions along the cortical hierarchy. Our results are in line with recent findings of representations with power-law spectra in the primary visual cortex (V1) of mice¹ (Stringer et al., 2019). Next, by aligning the activations of different subjects, we show that they share a common representation over many latent dimensions, suggesting that they represent the visual world using a similar scale-free code despite idiosyncrasies in brain anatomy and learning experiences. In contrast, we find that conventional RSA is only sensitive to leading, high-variance dimensions and thus fails to reveal the full extent of these shared population codes. Together, our results show that human visual cortex represents natural images in cortical population activity with a universal scale-free spectrum, and they reveal a rich space of stimulus-related dimensions that have been out of reach for conventional methods but may be critical for understanding the cortical code of human vision.

2 Results

We set out to study the statistical properties of stimulus-related fluctuations in the fMRI responses of visual cortex and to characterize the spectral properties of visual representations shared across individuals. To do so, we analyze the activation covariance, which captures all second-order (pairwise) interactions between voxels.

An important first step is to characterize the eigenvalue spectrum of this neural covariance, which describes how variance decays across dimensions. The spectral decay informs us about the fraction of dimensions that effectively contribute to the global variance, which is related to the smoothness of the representation. If the spectrum displays an exponential decay, this indicates that there is a finite effective dimensionality capturing most of the variance. In contrast, if a heavy-tailed distribution is observed, it is necessary to consider the full spectrum because the effective dimensionality may not have an intrinsic upper bound other than the total number of neurons, which is about 10^9 in human visual cortex.

Note that it is possible for individuals to have similar covariance eigenspectra but use different latent dimensions to encode images in distinct ways. Thus, it is necessary to go beyond characterizing the spectrum of stimulus-related variance *within* each individual and identify the degree to which this variance is shared *between* individuals. By directly examining shared variance, we can identify representational properties that are consistent across individuals and are likely to have a fundamental role in visual information processing.

We point out that standard principal component analysis (PCA) of cortical activations is not adequate to reach our goals as it decomposes all sources of variance, including both the stimulus-related signal of interest and noise. In addition, when comparing two individuals, we are considering two covariances expressed in different spaces, which could be rotated relative to one another or contain fundamentally different dimensions. Thus, cross-validation and functional alignment are needed to identify the shared stimulus-related information in cortical activity. Below we describe a method to achieve these goals.

¹We will present a comparative study of mice and humans in a companion paper.

2.1 A spectral method to estimate similarities between high-dimensional representations

Given a pair of subjects X and Y who have seen the same images, we investigate properties of their cortical representation covariances $\Sigma_k(X, X)$, $\Sigma_k(Y, Y)$ and their cross-covariance $\Sigma_k(X, Y)$ as a function of rank k from an orthogonal decomposition. To estimate the level of similarity between representations, our goal is to compute the correlation

$$r_k(X, Y) = \frac{\Sigma_k(X, Y)}{\Sigma_k(X, X)^{1/2} \Sigma_k(Y, Y)^{1/2}} \quad (1)$$

as a function of rank k for latent dimensions sorted by decreasing variance. The correlation function r_k characterizes the range of dimensions over which the representation in one subject is shared with another. For this ratio to be meaningful, it is important to estimate the numerator and denominator in the same statistical manner and take into account the following requirements:

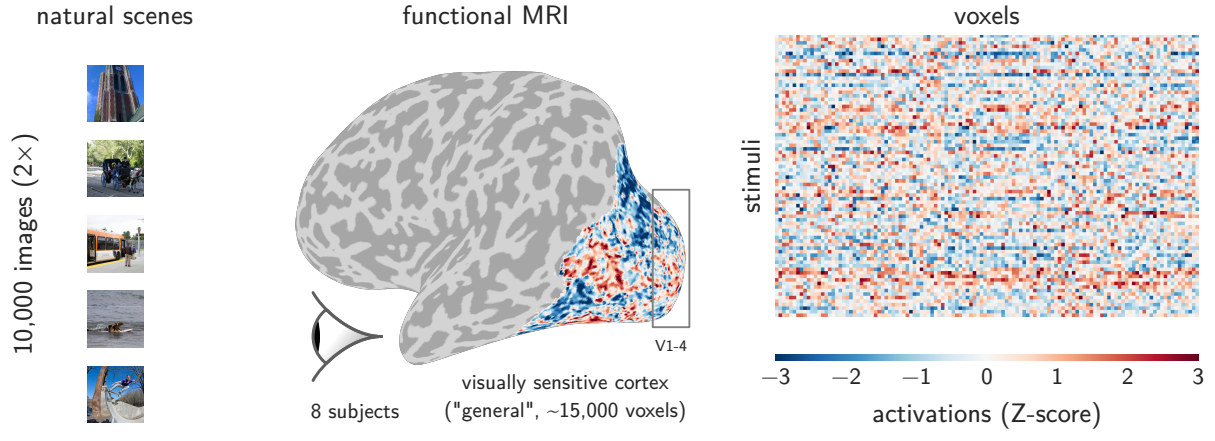
1. We want to consider only activations that are stimulus-dependent and discard others. This requires cross-validation of covariances using repeated stimulus trials. For between-subject comparisons, we average over cross-trial comparisons so that the estimator is insensitive to the order of the trials.
2. To characterize the shared dimensions of different subjects, the representations need to be hyperaligned by solving the Procrustes problem, which finds the optimal rotation for aligning two matrices along shared latent dimensions (Haxby et al., 2011).
3. We are interested in results that generalize and do not reflect chance alignments of a particular dataset. To do so, we systematically use cross-validated train/test splits in our spectral estimation. This cross-validation ensures that if the data are random, the expected covariance estimates will be zero rather than being all positive, as in a standard orthogonal decomposition.

We refer to this procedure as cross-decomposition. It uses the orthogonal rotation method from hyperalignment to align representations along a set of shared latent dimensions (Haxby et al., 2011). A set of training data is used to learn these orthogonal transformations. Once the representations are aligned, we compute cross-validated covariance estimates along each latent dimension using held-out test data, yielding a cross-covariance singular value spectrum. In sum, the cross-validated singular values from this procedure reflect shared stimulus-related variance that is reliably detected in held-out data. We present a detailed mathematical formalism of these estimators in the Methods section. The main steps are also illustrated in Figure 1.

We note that while this approach shares similarities with the covariance eigenspectrum obtained by cross-validated PCA (cvPCA), it also departs from it in two important ways (Stringer et al., 2019). First, cvPCA can only be applied to within-subject analyses. To explore the level of shared representations between subjects, we need a method that can meaningfully align their representations. Second, cvPCA examines reliability across stimulus repetitions for a set of images but does not examine generalization to new images. Because our goal is to characterize representational properties that generalize over images, our cross-decomposition approach assesses both reliability across stimulus repetitions *and* generalization to new stimuli. As a result of these differences, cross-decomposition and cvPCA characterize different statistical quantities whose spectra naturally differ. This is illustrated in Figure 1, where standard PCA, cvPCA, and cross-decomposition exhibit different spectral decays due to their different generalization requirements. Note that an important consequence of this is that the power-law slopes observed for different estimators should not be directly compared.

Finally, we highlight two important considerations for characterizing high-dimensional representations:

1. **A spectral approach** is needed to assess the nature of representations in their full extent and to meaningfully compare high-dimensional quantities. A spectral approach allows us to determine if representations are localized over a finite range of dimensions or spread over an unbounded range (in practice limited by the dataset), and it allows us to compare individuals across all underlying dimensions of cortical activity. We point out that other approaches for comparing representations, such as RSA and centered kernel alignment, typically extract a single scalar coefficient of similarity that is variance-weighted (Kornblith et al., 2019; Kriegeskorte, 2008). As a result, they are effectively dominated by a relatively limited number of low-rank dimensions and are not sensitive



- 1 Learn the latent dimensions shared between two sets of neural responses on training data

$$\begin{aligned} \text{cov}(X_{\text{train}}, Y_{\text{train}}) &= X_{\text{train}}^T Y_{\text{train}} / n_{\text{train}} \\ &= U_{\text{train}} \Sigma_{\text{train}} V_{\text{train}}^T \end{aligned}$$

- 2 Compute the spectrum of variance along the latent dimensions on held-out **test data**

$$\begin{aligned} \Sigma_{\text{test}} &= \text{cov}(X_{\text{test}} U_{\text{train}}, Y_{\text{test}} V_{\text{train}}) \\ &= (X_{\text{test}} U_{\text{train}})^T (Y_{\text{test}} V_{\text{train}}) / n_{\text{test}} \end{aligned}$$

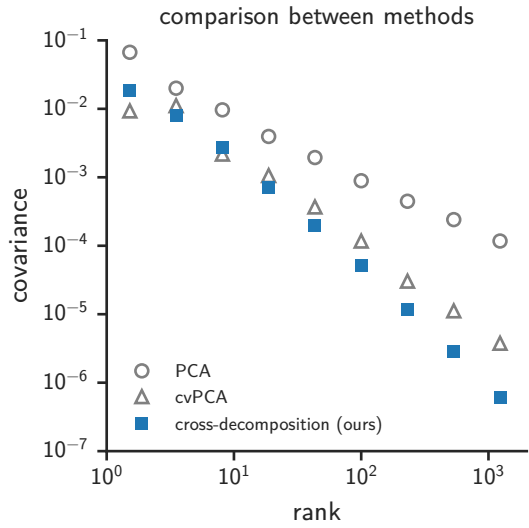


Figure 1: Cross-decomposition procedure to estimate the cross-validated spectrum of visual representations. (Top) Each participant viewed about 10,000 natural scene images multiple times while their fMRI BOLD responses were measured. The depicted brain region is a “general” region of interest in visual cortex that was identified by selecting all voxels whose activity was modulated by the presentation of images. (Bottom) Estimating a cross-validated covariance spectrum requires identifying directions of variance that are shared between two sets of cortical responses given a set of training images. Sets can have repeated presentations of stimuli to a single subject or repeated presentations of the same stimuli to two different subjects. The reliable shared variance is then evaluated on cortical responses to held-out test images. Example spectra are shown for subject 1 based on our cross-decomposition approach as well as PCA and cvPCA.

to potentially many informative high-rank dimensions. We illustrate this point in Figure S7, which is discussed in detail in Section 2.4. To explore high-dimensional properties of neural representations, it is necessary to take a spectral approach and estimate quantities as a function of rank k obtained from an orthogonal decomposition. As described in Equation 1, our goal is therefore to estimate a correlation function r_k rather than a single scalar coefficient.

2. **Aggregating latent dimensions** by binning the statistical estimates in our spectra can provide substantial gains in sensitivity, allowing us to measure spectral shape well beyond the range over which individual components are detected. This comes at the cost of lowering the resolution at which we characterize the latent space of the system, but, if the spectrum presents a smooth dependence on rank, this aggregation can reduce noise with a negligible loss of information. Such an approach is ubiquitous in physics. In contrast, previous work in neuroscience has often focused on latent dimensions that can be individually detected (and, if possible, interpreted). When focusing on individual dimensions, the unavoidable presence of noise imposes severe limitations on the range of dimensions that can be studied and effectively limits such an approach to a low-dimensional view of neural representation. Here, our goal is to probe the statistical structure of activation covariances and characterize the full extent of the spectrum of visual representations and their similarities between individuals.

2.2 Scale-free representations in visual cortex

We first used our cross-decomposition approach to characterize, as broadly as possible, the spectrum of image representations in a general region of interest (ROI), including all visually responsive voxels. The results are presented in the left panel of Figure 2. Interestingly, despite focusing on only stimulus-related variance that generalizes to held-out data (i.e., putting strong requirements on the selected variance), we can reliably detect signals following a power-law distribution across four orders of magnitude of latent dimensions. As described in the methods section, we normalized the overall amplitude of covariances to account for the varying number of voxels between individuals (see Figure S1). The error bars in Figure 2 depict variance across cross-validation folds, demonstrating that the covariance statistics are reliably estimated. Furthermore, in Figure S3, we performed permutation tests by randomly shuffling images before computing the covariance estimates, allowing us to further demonstrate that the observed covariance spectrum is statistically significant over a wide range of ranks.

These findings have several key implications. First, they demonstrate that human visual cortex represents natural images in population activity that is *scale-free*. The scale-free nature of these representations implies that their dimensionality is ill-defined: estimates of effective dimensionality for visual cortex likely reflect the properties of a given dataset (i.e., the number and richness of stimuli, the number of recording channels) rather than an intrinsic property of cortical representation. In fact, our findings suggest that the representations of visual cortex are expressed over *all* available dimensions and that, given the power-law behavior, any low-rank truncation of these representations would lead to a non-negligible loss of stimulus-related information. Given that the maximum reachable rank is commensurate with the number of neurons in visual cortex, the neglected information could be immense. Second, the observed consistency of these spectra across subjects shows that there is universality in how variance is spread across latent dimensions in different individuals. In other words, visual cortex representations have the same level of smoothness across people.

We also observed that the typical spatial scales over which fMRI signals fluctuate decrease with rank. This is illustrated in Figure S2. This suggests that the scale-free property of cortical representations exists over a wide range of physical scales, from tens of centimeters down to the limiting resolution of the experiment (i.e., 1.8 mm). Interestingly, similar scale-free covariance spectra have been reported in the primary visual cortex of the mouse brain (Stringer et al., 2019). These results are based on calcium imaging measurements of individual neurons (i.e., on physical scales several orders of magnitude smaller than the ones used in our fMRI analysis). Together, our findings and the previous findings in mice point to a possible ubiquity of scale-free activation spectra in mammalian visual cortex. Note that, as mentioned above, the power-law exponents of the mouse spectra from Stringer et al. (2019) and the human spectra reported here cannot be directly compared, as they are based on different statistical estimators. In a companion paper, we will present direct quantitative comparisons of the spectra in humans and mice.

In summary, our results show that visual cortex representations are expressed over several orders of magnitude of latent dimensions and display a universal scale-free spectrum. While the variance is dominated by a subspace substantially smaller than the entire space, the scale-free nature of the spectrum suggests that its dimensionality is ill-defined and likely unbounded (up to the number of neurons).

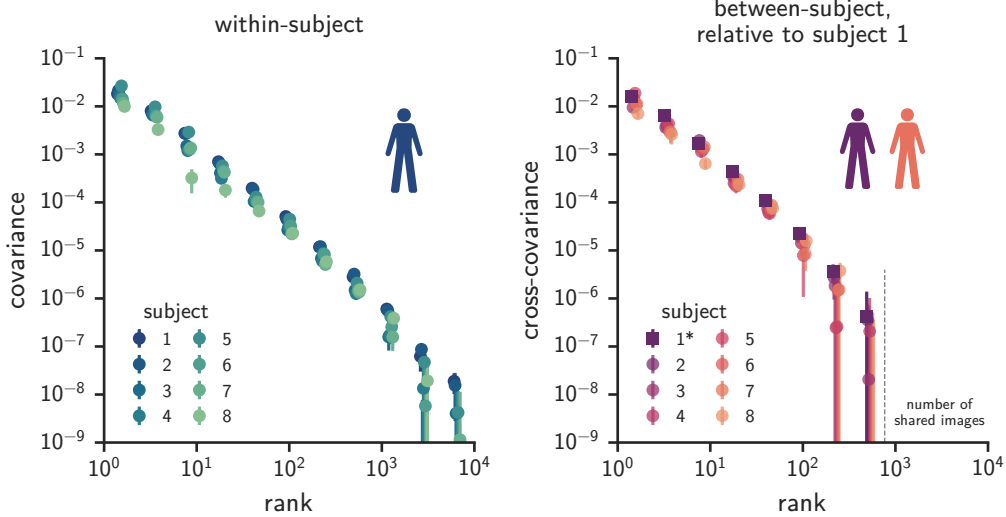


Figure 2: Cortical representations of natural images are scale-free and shared across subjects over many dimensions. (Left) Within-subject covariance spectra of visual cortex responses in a general region of interest including all visually responsive voxels from the Natural Scenes fMRI dataset (Allen et al., 2021). (Right) Between-subject covariance spectra for the same region of interest, characterizing shared variance relative to reference subject 1. The range is limited by the number of shared stimuli seen by all subjects. All spectra are normalized to account for differences in the number of voxels across participants and averaged within bins of exponentially increasing width and across 8 folds of cross-validation. Error bars denote standard deviations across these 8 folds. Figure S4 shows the results of the same analysis using each subject as the reference subject.

2.3 A representational code shared across individuals

We next explore whether representational dimensions are shared *between* individuals (i.e., whether their latent dimensions co-vary for the same stimuli). Representations can be compared across subjects using methods like RSA (Kriegeskorte, 2008) or hyperalignment (Haxby et al., 2011), with the latter enabling comparisons of individual dimensions across subjects. This hyperalignment is achieved by our cross-decomposition technique. We use it to estimate the cross-covariance spectrum between individuals $\Sigma_k(X, Y)$ for the available subset of approximately 1,000 images which were shown to all participants in the Natural Scenes Dataset experiment.

The right panel of Figure 2 shows the results for comparisons relative to subject 1. In this figure, the square symbols represent the within-subject spectrum for subject 1 (as in the left panel), and the circles represent comparisons with other subjects. This analysis reveals that the between-subject spectra are remarkably similar to the within-subject spectrum—again exhibiting a scale-free power-law distribution that spans nearly three orders of magnitude of latent dimensions. Comparisons between all other pairs of subjects yielded similar results and are shown in Figure S4. Permutation tests again showed that the observed covariance spectra are robustly detected across many ranks (Figure S3). Note that the upper bounds of these spectra are limited by the size of the available dataset—we expect that with more stimuli, even more shared dimensions would likely be revealed.

As shown in Figure S5, if we rely on anatomical alignment alone and assume that subject-specific rotations are irrelevant, we only detect shared variance up to about ten dimensions. Thus, while these dimensions may have similar coarse-scale anatomical properties across individuals, shared dimensions at higher ranks require subject-specific functional alignment to be detected.

In sum, these results show that visual representations co-vary between subjects over many ranks of dimensions, and they suggest that despite differences in experience and cortical anatomy, the visual cortices of different individuals converge to a universal scale-free code for natural image representation.

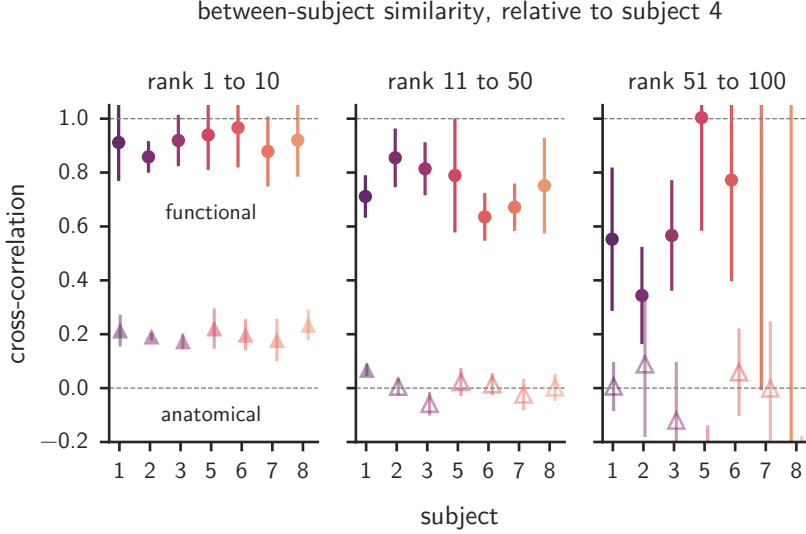


Figure 3: Representational similarity in visual cortex for pairs of subjects. Correlation of neural representations as a function of ranks obtained from the ratio of cross-validated between-subject variance relative to cross-validated within-subject variance (Equation 1). These findings show that the stimulus-related variance in cortical activity is largely shared across subjects over many ranks. Furthermore, the similarity of high-rank dimensions can only be detected when the representations are functionally aligned in a shared space using subject-specific rotation matrices. With anatomical alignment alone, shared representations are undetectable beyond ≈ 10 dimensions. Error bars denote standard deviations across 8 folds of cross-validation. Open symbols denote points where the mean is less than three standard deviations above zero. Figure S6 shows the results of the same analysis using each subject as the reference subject.

2.4 Similarity of scale-free representations

We next address a central question about the nature of shared representations: To what degree are neural representations shared between individuals? Having performed spectral decomposition of both the within-subject and between-subject covariances, we can now compare the ratio of these covariance estimates to determine the proportion of stimulus-related variance that is shared between individuals. Specifically, we compute the set of correlation coefficients $r_k(X, Y)$ between subjects as a function of rank (Equation 1). Being ratios, these correlation coefficients are expected to be noisier than the corresponding covariance spectra. To ensure a sufficiently high signal-to-noise, we aggregated these ratios over wider bins of ranks than used above.

As shown in Figure 3, our analysis reveals a high level of correlation over a range of latent dimensions, a finding that is consistent for all subjects considered in the analysis. While we can only detect the correlations among subjects over two orders of magnitude in ranks, our observation of universal power-law distributions in both the within-subject and between-subject spectra suggests that this correlation likely holds well beyond this range (Figure 2). This prediction can be tested in the future with larger datasets. It is also worth noting that while these plots show a remarkable degree of similarity across subjects, some level of subject-specific stimulus-related variance gradually emerges with ranks. An intriguing question for future work is to investigate whether this subject-specific variance reflects meaningful individual differences in visual processing and to determine whether individual differences reliably increase as a function of latent-dimension rank.

As mentioned above, our cross-decomposition approach together with a spectral analysis were critical for revealing the high-dimensional nature of these shared representations. Specifically, to meaningfully compare population activity between subjects, it is necessary to *functionally* align their representations into a shared space by applying hyperalignment (i.e., subject-specific rotation matrices) (Haxby et al., 2011). If we use anatomical alignment alone and assume that subject-specific rotation matrices are not needed, we only detect representational similarity for the first ten dimensions, as shown by the triangle symbols in Figure 3. In addition, it is important to note that variance-weighted estimators (without any spectral decomposition) are mainly sensitive to low-rank dimensions and therefore

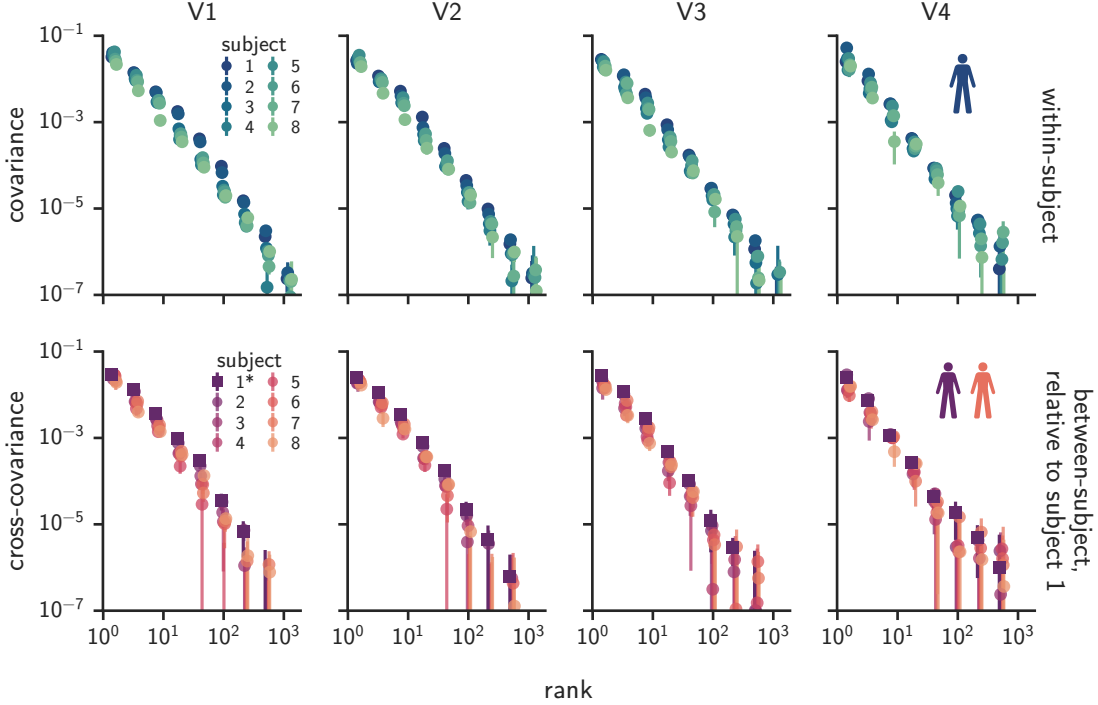


Figure 4: Scale-free representations are consistently observed across multiple regions of visual cortex. These plots show within-subject (top) and between-subject (bottom) covariance spectra for retinotopic regions along the visual hierarchy from V1 to V4. In comparison with the larger region of interest shown in Figure 2, these findings demonstrate that the same scale-free power-law distribution is observed in smaller regions of interest, and they show that these power-law distributions are highly consistent across regions. This implies that across these regions of the visual hierarchy, there is universality in the smoothness of cortical population codes. Further, the between-subject spectra show that each of these regions represents images using high-dimensional codes that are shared across individuals. Error bars denote standard deviations across 8 folds of cross-validation.

not adequate to probe the properties of high-dimensional representations. We found that a conventional implementation of RSA is effectively sensitive to only a handful of latent dimensions and cannot distinguish between low- and high-dimensional representations, as demonstrated in Figure S7. Furthermore, visualizations show that the low-rank dimensions detected with anatomical alignment and RSA correspond to coarse-scale gradients of cortical tuning, as shown in Figure S2. Thus, the conventional methods of cognitive neuroscience provide a view of neural representation that is effectively low-dimensional and spatially coarse.

In sum, these findings show that the stimulus representations of visual cortex are not only scale-free but also encode similar information in the brains of different individuals. Most of these representational dimensions have subject-specific anatomical properties, making them undetectable with anatomical alignment alone, and they are obscured in the representational similarity matrices of RSA—functional alignment and spectral analyses are necessary for revealing these shared dimensions. The shared nature of these representations implies that the entire spectrum of activity contributes to the sensory code. This suggests that there is a wealth of representational content in measurements of visual cortex that has remained beyond the reach of conventional methods but may be crucial for understanding human vision.

2.5 Consistent behavior across visual cortex regions

After first focusing on a large and general ROI of visually responsive voxels, we next investigate whether our findings are representative of the structure of population codes observed across different visual regions. To answer this question, we computed both the within- and between-subject cross-decomposition spectra for the retinotopic regions V1, V2, V3, and V4. As shown in Figure 4, we found the spectra in these regions to be highly similar to the spectra observed

for the general ROI, despite these retinotopic ROIs being much smaller in size. This is observed for both the within-subject and between-subject cross-decomposition analyses. This finding suggests that there is spatial-scale invariance in the power-law spectrum of visual cortex activity: a consistent power law is observed when considering a large general ROI of all visually responsive voxels or when considering much smaller retinotopic ROIs. Furthermore, these findings show that the spectra are highly consistent across regions, which means that we do not find evidence for either dimensionality reduction or expansion along consecutive stages of visual processing. Thus, at least up to mid-level visual regions (i.e., V4), the representations of visual cortex exhibit a universal scale-free format with a characteristic power-law index.

3 Discussion

3.1 The nature of neural representations

Key results We found that the population codes of human visual cortex are scale-free and, to a great extent, shared among individuals. Scale-free cortical activity patterns represent sensory information using the full range of their latent dimensions, and this sensory information is largely shared across subjects. Due to their scale-free nature, these representations cannot be reduced without discarding reliable sensory signal and attempts to quantify their effective dimensionality depend on the size of the dataset. We observe stimulus-related variance to decay across the principal axes of these population codes according to a characteristic power-law distribution. The same power law was observed in all subjects, in multiple regions along the visual hierarchy, and at multiple spatial scales, which suggests that there is a fixed balance between the contributions of low- and high-rank dimensions in the cortical code for vision. In short, these findings reveal a universal scale-free representation of natural scenes in the human brain.

Though many previous studies have examined visual representations in human and monkeys through the lens of dimensionality reduction (e.g. Khosla et al., 2022; Lehky et al., 2014), recent results obtained from calcium imaging of the mouse brain have revealed scale-free power-law distributions over at least two decades of ranks in the cross-validated covariance spectra of cortical populations (Manley et al., 2024; Stringer et al., 2019). The specific power-law exponents from these studies and ours cannot be compared directly due to differences in statistical estimators (as illustrated in Figure 1). We will present direct quantitative comparisons of the mouse and human spectra in a companion paper. Nonetheless, these studies in mice and our work in humans demonstrate convergent findings of scale-free structure in cortical activity patterns measured at vastly different spatial resolutions, and they suggest that scale-free population codes may be a general representational strategy of mammalian cerebral cortex.

Implications for neural mechanisms The observation of a consistent spectral behavior across individuals, brain regions, spatial scales, and possibly species is a strong indication that a simple, generic neural mechanism is at play, likely to arise from principles of network self-organization. It is important to understand its nature as it speaks to the fundamental principles that govern the activity and computations of neural populations. Previous work suggests several possible hypotheses, which are not mutually exclusive. It has been proposed that power-law covariance eigen-spectra emerge in neural populations that strike an optimal balance between expressivity and robustness (Stringer et al., 2019). Along these lines, Prince et al. (2024) showed that when the covariance eigenspectra of artificial neural networks are made to achieve this balance through regularization during learning, they exhibit a better representational match to human visual cortex. Using connectivity arguments, Lynn et al. (2024) showed that a Hebbian learning mechanism yields heavy-tailed neuronal connectivity distributions which, under certain conditions, may lead to scale-free covariance spectra. One appeal of such a Hebbian learning account is that it does not require goal-directed feedback (i.e., backpropagation). An exciting direction for future work is to identify which principles govern the underlying mechanism leading to the scale-free representations of mammalian cerebral cortex.

Previous work has argued that the level of dimensionality in a brain region is linked to the region's functional specialization, with some functions calling for high dimensionality and others low dimensionality (e.g. Cayco-Gajic & Silver, 2019; Fusi et al., 2016). In the case of vision, there have been conflicting proposals about the link between dimensionality and visual information processing. Some have argued for the importance of dimensionality *expansion* to improve linear separability of stimulus classes (Babadi & Sompolsky, 2014; Elmoznino & Bonner, 2024). Others have argued for the importance of dimensionality *reduction* to suppress irrelevant variance and yield robust representations of behaviorally relevant variables (Ansuini et al., 2019; Cohen et al., 2020; Fusi et al., 2016; Lehky & Tanaka, 2016). However, our findings suggest that natural image representations neither expand nor contract along successive stages

of the visual hierarchy, at least up to mid-level representations. Instead, we observe a remarkable degree of stability in the power-law structure of visual population codes. An important question for future work is whether differences in dimensionality may emerge in downstream regions that support higher-level visual cognition.

Prior investigations have shown that visual cortex representations are at least partly shared across people and species (Haxby et al., 2011; Kriegeskorte, 2008) and that hyperalignment is critical for uncovering the common dimensions that underlie these shared representations (Haxby et al., 2011, 2020). Our work pushes this exploration further by showing that the shared representations are scale-free: they are expressed over all dimensions and only limited by the size of the data. Furthermore, we quantified the portion of stimulus-related variance within each subject that is shared with others, and we found that, remarkably, this variance is shared over a wide range of ranks. This means that across the range considered in this analysis, images are represented in a similar way in the brains of different individuals. Thus, despite differences in experience and brain anatomy, the human visual system appears to converge to a common high-dimensional code for natural images.

As in previous work (Haxby et al., 2011), our findings show that the shared representational dimensions of different brains can only be fully observed by hyperaligning the cortical activity patterns from one individual to another. This implies that the underlying dimensions of the representational code are not spatially localized but instead correspond to latent dimensions that are distributed. Although the brain clearly exhibits spatially localized functions on large scales (e.g., the visual cortex is well localized), our results indicate that when examining brain activity on progressively smaller scales, the representations become more distributed. Indeed, we only found evidence for shared spatial localization in the first decade of the representational spectrum, with the bulk of stimulus-related information expressed through universal latent dimensions that have distinct spatial distributions in each subject and require subject-specific rotation matrices. An important goal for future work is to understand what kind of learning mechanism can explain how the human brain converges to a shared representational code over many dimensions despite subject-specific spatial organization. Some insight might come from studies of artificial neural networks, which also exhibit universal learning properties that can be detected in their latent dimensions rather than their neurons (e.g. Chen & Bonner, 2024; Guth & Ménard, 2024).

Limitations of our analysis In this work, we explored the properties of neural representations using linear methods, based on an orthogonal decomposition of variance in all directions, with a generalization test in held-out data. This linear description of activations is appealing as it characterizes the information that could be decoded by downstream neurons implementing a simple linear readout procedure, which is a key motivation for the usefulness of this approach. However, it is possible that nonlinear mappings of representations could provide lower-dimensional descriptions of visual cortex activity (Ansini et al., 2019; De & Chaudhuri, 2023; Jazayeri & Ostoic, 2021). If so, the shared representation between individuals could potentially be an intrinsically lower dimensional object. An exciting direction for future work is the pursuit of cross-validated nonlinear dimensionality methods that can allow for direct comparisons of linear and nonlinear dimensionality measurements of stimulus-dependent variance.

3.2 Comments on traditional approaches in cognitive neuroscience

The “low-resolution” view of variance-weighted estimators in neuroscience The scale-free nature of sensory representations observed here has important implications for the methods of neuroscience. First, it is a common practice to examine neural representations through dimensionality reduction (Cunningham & Yu, 2014; Haxby et al., 2011; Huth et al., 2012; Khosla et al., 2022; Lehky et al., 2014). In such approaches, researchers typically invoke a criterion to identify a subset of “signal” dimensions that account for much of the variance in the data, while discarding the remaining dimensions, which are considered either unimportant or noise-dominated. However, a robust estimate of the covariance spectrum reveals a power-law distribution rather than a distribution with an exponential cutoff. This implies that there is no intrinsic upper bound on the “signal” dimensions, and it suggests that while typical dimensionality-reduction methods may account for much of the *variance*, they discard much of the *information*, which can be found in the long tail of low-variance but nonetheless reliable dimensions. Another important implication is that typical *variance-weighted* estimators, including RSA, voxelwise encoding models (i.e., regression), and linear classifiers, are insensitive to the full extent of information in a power-law distribution. Instead, these methods exhibit a sensitivity to latent dimensions that decays rapidly with rank and becomes vanishingly small beyond the first decade of ranked dimensions. Thus, the correlation metrics obtained with these methods are unable to fully capture the richness of representations expressed in high dimensions. We demonstrate this point in Figure S7 by presenting RSA analyses of representations in low and high dimensions, which show that this technique is effectively insensitive to the effects from

ranks greater than about 10. Moreover, because low-rank dimensions correspond to large-scale cortical gradients, this means that typical variance-weighted methods, like RSA, effectively view neural representations through a spatially low-resolution lens. This suggests that there is a vast space of uncharted dimensions in neural activity that has been out of reach for conventional methods and whose role in human cognition has yet to be thoroughly investigated.

Limitations of brain maps and semantic interpretations Another consideration raised by our findings is that common methods used for visualizing and interpreting neural representations are severely limited in their ability to characterize high-dimensional information. One such method is brain mapping, which cognitive and systems neuroscientists use to characterize the spatial organization of response preferences to representational dimensions (Bao et al., 2020; Contier et al., 2024; Hebart et al., 2023; Huth et al., 2012; Tarhan & Konkle, 2020). One brain map can only convey a small number of representational dimensions. However, as we have shown, human brain representations are expressed using the full dimensionality of the available space (ultimately defined by the number of neurons) and through a scale-free activation spectrum. An unrealistic number of brain maps would be needed to convey the robust high-dimensional sensory information that our spectral analysis reveals. As a result, brain map visualizations can only scratch the surface of neural representations and cannot illuminate the full extent of the reliable information in cortical population activity. Furthermore, because of the need to hyperalign subjects to find their shared dimensions, the common approach of averaging fMRI results over anatomically aligned brains effectively limits our view to the relatively small number of dimensions whose anatomical distributions are highly similar across subjects. We suggest that understanding neural representations in their entirety requires a transition from a localized, map-based view of the brain to a more distributed statistical description that considers the full spectrum of the cortical code.

A similar consideration applies to the semantic interpretation of representational dimensions, which is typically restricted to low-rank dimensions that can be individually detected without the need for spectral binning (Hebart et al., 2023; Huth et al., 2012; Khosla et al., 2022; Tarhan & Konkle, 2020). As we showed, aggregating dimensions allows one to dramatically extend the range over which latent dimensions are detectable. Such a binning procedure, though common in other fields that examine power-law distributions (Lin & Newberry, 2023), has not typically been used in studies of neural representation. Doing so requires that we focus on the spectrum as a whole rather than seeking to interpret each latent dimension. Intriguingly, scale-free properties can be found in multiple aspects of the brain, as previous studies have detected scale-free power-law distributions in temporal activity patterns, structural connectivity, and behavior (He, 2014; Kello et al., 2010; Lynn et al., 2024). This suggests that methods for rigorously characterizing phenomena distributed over many orders of magnitude may prove crucial to understanding the human brain. To be clear, we believe that the visualization methods of previous work have revealed important organizing properties of the brain. However, if we want to move beyond low-dimensional characterizations of neural representation, we need to embrace approaches for exploring representations in their full extent and understanding them mathematically rather than visually or semantically (Roads & Love, 2024).

3.3 Summary

Together, our findings reveal the scale-free format of the cortical code for human vision. We found that natural images evoke reliable variance with a power-law spectrum across multiple orders of magnitude of latent dimensions. Importantly, we also found that a large number of these dimensions are shared across individuals, suggesting a remarkable degree of convergence despite individual differences in neuroanatomy and experience. To obtain a global view that captures more than the first ~ 10 dimensions, it is crucial to use both spectral analysis and functional alignment. Otherwise, one is typically limited to high-variance dimensions (as is the case for RSA) or the subset of dimensions that tend to be anatomically aligned. In sum, these findings suggest that the sensory code of visual cortex spans all available dimensions of population activity and that fully understanding human brain representations requires a high-dimensional statistical approach.

4 Methods

4.1 Dataset

Experimental design We used the Natural Scenes Dataset (NSD), a large-scale 7T fMRI dataset of image-evoked blood-oxygen-level-dependent (BOLD) responses to approximately 10,000 stimuli in each of eight participants. The stimuli were taken from the Common Objects in Context (COCO) image dataset, and they contain photographs of a large and diverse set of objects in their natural scene contexts. Participants viewed these images in the scanner while performing a recognition memory task (i.e., “Have you seen this image before?”). Images were shown three times over the course of the experiment, and trial-level response estimates were obtained for $\sim 30,000$ stimulus presentations (about 10,000 images \times 3 trials per image). A subset of 1,000 images were seen by all participants in the experiment while the remaining images were unique to each participant. However, note that some participants did not complete all scan sessions and, thus, had fewer stimulus trials.

Data preprocessing We used the 1.8 mm volumetric preparation of the data, with version b2 of the betas (betas_fithrf), which were z-scored within each scanning session to reduce non-stationarity, as recommended by the authors. We refrained from using the denoised version b3 of the betas (betas_fithrf_GLMdenoiseRR) since (i) the dimensionality reduction applied by the denoising might remove reliable low-variance signal and (ii) these betas were specifically optimized to maximize reliability across trials, which could bias our analyses of reliable cross-trial variance.

Regions of interest For our main analyses, we focused on a pre-defined “general” region of interest (ROI), which included all stimulus-responsive voxels in visual cortex (i.e., the large “nsdgeneral” ROI ranging in size from 12,000 to 18,000 voxels across subjects). We also performed follow-up analyses in smaller ROIs (i.e., the retinotopic regions V1, V2, V3, and V4) to explore possible changes along the visual processing stream.

4.2 Formalism

Given the representations of n stimuli in two different systems, the neural responses can be organized into two data matrices $X \in \mathbb{R}^{n \times d_X}$ and $Y \in \mathbb{R}^{n \times d_Y}$ where the rows correspond to n presented stimuli and the d_X, d_Y columns correspond to the numbers of recording channels — here, voxels from functional neuroimaging. Our goal is to characterize the similarities between the representations of two neural systems. We do so by characterizing their neural representation covariances $\Sigma_k(X, X)$ and $\Sigma_k(Y, Y)$ and the cross-covariance $\Sigma_k(X, Y)$ as a function of rank k from an orthogonal decomposition. The similarity can then be quantified by the spectral correlation

$$r_k(X, Y) = \frac{\Sigma_k(X, Y)}{\sqrt{\Sigma_k(X, X)\Sigma_k(Y, Y)}}.$$

4.3 Computing within-subject spectra $\Sigma_k(X, X)$

To robustly estimate the covariance spectrum Σ_k of neural responses to stimuli, we compute the cross-covariance of neural responses to the same images on different trials, say X_1 and X_2 , which ensures that the estimated covariance generalizes across repeated presentations of the stimuli. Additionally, we cross-validate the covariance spectra across images to ensure that we extract stimulus-related variance and not stimulus-independent noise.

Specifically, we split X into *training* and *test* sets X_{train} and X_{test} , compute the singular value decomposition of the cross-covariance of the training data

$$\text{cov}(X_{1,\text{train}}, X_{2,\text{train}}) = n^{-1} X_{1,\text{train}}^\top X_{2,\text{train}} = U_{\text{train}} \Sigma_{\text{train}} V_{\text{train}}^\top$$

and evaluate the reliable variance along each latent dimension by projecting the test data onto the singular vectors U_{train} and V_{train}

$$\Sigma(X_1, X_2) = \text{cov}(X_{1,\text{test}} U_{\text{train}}, X_{2,\text{test}} V_{\text{train}}) / d_X$$

where the normalization by d_X (number of voxels) enables meaningful comparisons between representations with different numbers of channels (see Figure S1 for more detail). All the data are centered using the mean of the training sets.

When the train and test samples are drawn from the same distribution, the covariance matrix Σ is diagonal in expectation. In practice, under normal circumstances, Σ is quasi-diagonal and we have verified that the contribution from off-diagonal terms is negligible. We thus estimate the cross-validated spectrum as

$$\hat{\Sigma}_k(X, X) = \text{diagonal of } \Sigma(X_1, X_2).$$

Cross-validation scheme To use all available data, we divide the stimuli into 8 folds, then use 7 folds to learn singular vectors and the remaining fold to estimate variance along the dimensions. Specifically, X_{train} has 7 times as many stimuli as X_{test} . We repeat this process 8 times using each fold as the test set once, producing eight spectra. Finally, we average the binned spectra across all 8 folds to obtain $\hat{\Sigma}_k$.

4.4 Computing between-subject spectra $\Sigma_k(X, Y)$

When computing *between-subject* spectra, X_i contains neural responses from subject X on the i^{th} presentation of the shared stimuli while Y_j contains neural responses from subject Y on the j^{th} presentation of the shared stimuli.

We compute the singular value decomposition of the cross-covariance between the two training sets of neural responses

$$\text{cov}(X_{i,\text{train}}, Y_{j,\text{train}}) = n^{-1} X_{i,\text{train}}^\top Y_{j,\text{train}} = U_{\text{train}} \Sigma_{\text{train}} V_{\text{train}}^\top$$

and evaluate the covariance that generalizes to held-out stimuli by projecting the test sets onto the singular vectors U_{train} and V_{train}

$$\hat{\Sigma}_k(X_i, Y_j) = \text{diagonal of } \text{cov}(X_{i,\text{test}} U_{\text{train}}, Y_{j,\text{test}} V_{\text{train}}) / \sqrt{d_X d_Y}$$

where the normalization by the geometric mean of the number of voxels d_X and d_Y enables meaningful comparisons between the spectra for different pairs of subjects.

Since the ordering of trials is arbitrary, we make the estimated spectrum symmetric by averaging the spectra for two pairs of trials: (i) X_1 and Y_2 and (ii) X_2 and Y_1 , making our final estimate of the spectrum

$$\hat{\Sigma}_k(X, Y) = \frac{1}{2} [\hat{\Sigma}_k(X_1, Y_2) + \hat{\Sigma}_k(X_2, Y_1)].$$

Similar to our procedure for the within-subject spectra, we divide the stimuli into 8 folds and estimate cross-validated binned spectra.

Note that for all of these spectral analyses, the test singular values $\hat{\Sigma}_k(X, X)$ and $\hat{\Sigma}_k(X, Y)$ are not guaranteed to be positive, unlike a typical singular value spectrum. In fact, if the two systems share no reliable covariance that generalizes from the training set to the test set along a particular singular vector, the expected value of the corresponding test singular value is 0. We make use of this property to perform the null test shown in the inset of Figure S3.

Functional vs anatomical alignment In the lower panels of Figure 2, we refer to the between-subject spectra described above as *functionally* aligned spectra since they are computed by decomposing a cross-covariance matrix that assumes no anatomical alignment between the voxels across individuals. If we assume that different subjects' cortical surfaces are in fact anatomically aligned, i.e. the voxels at the same location in different subjects have identical tuning properties, we would expect that the latent dimensions from one participant should generalize to another. Specifically, we would expect that the rotation matrices U_{train} and V_{train} corresponding to the first and second subjects respectively could be swapped without losing any information when estimating cross-validated covariance on the test data.

We thus compute *anatomical* spectra by projecting X_{test} onto V_{train} instead of U_{train} and Y_{test} onto U_{train} instead of V_{train} and computing the covariance of the resulting projections. Since this procedure requires that the columns U_{train} and V_{train} correspond to the same anatomically aligned voxels across both subjects, we map all the neural responses onto

the standard Montreal Neurological Institute (MNI) space, downsample them to isotropic 1.8 mm voxels that match the resolution of the original dataset, and restrict our analyses to the common voxels that are present in both individuals. Both the *functional* and *anatomical* spectra are computed on these data to ensure that they are directly comparable.

4.5 Representational similarity analyses

Representational similarity matrices (RSMs) were constructed for each subject by computing Pearson correlations between patterns of fMRI responses to pairs of images and repeating this for all image pairs (using single trial-level responses from the “nsdgeneral” region of interest for each image, exactly as in the between-subject cross-decomposition analyses shown in the right panel of Figure 2). RSA correlations were obtained by correlating the RSMs for two subjects using either the linear (Pearson) or rank-order (Spearman) correlation coefficient. This procedure reflects a standard approach for comparing the representations of two individuals or an individual and a model. It is representative of a broader class of variance-weighted similarity metrics that also includes regression-based encoding models (Kornblith et al., 2019; Kriegeskorte & Diedrichsen, 2019).

Code availability All code for these analyses are available at this git repository.

5 Acknowledgments

This research was supported in part by a Johns Hopkins Catalyst Award to MFB, Institute for Data Intensive Engineering and Science Seed Funding to MFB and BM, and grant NSF PHY-2309135 to the Kavli Institute for Theoretical Physics.

Supplementary Figures

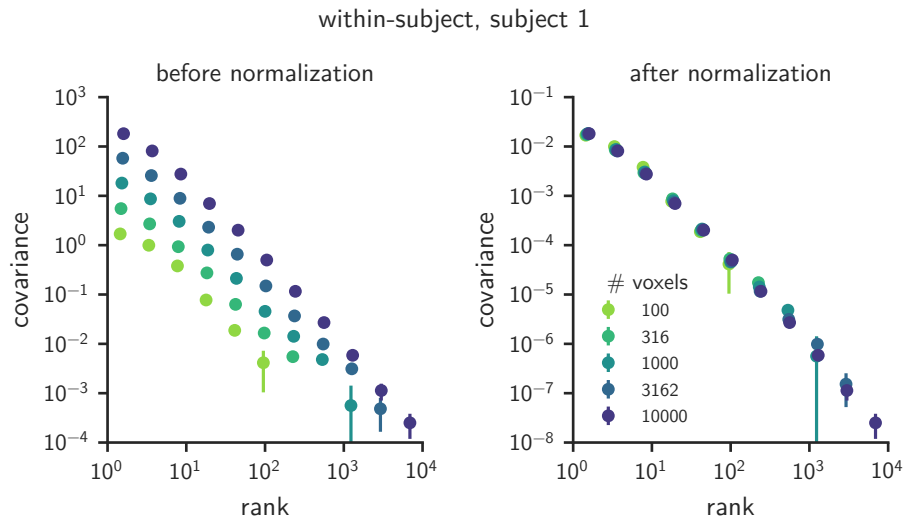


Figure S1: **Spectral normalization** (Left) Within-subject cross-trial spectra were computed with different numbers of voxels sampled from the general region of interest. Increasing the number of voxels leads to higher variance. (Right) Normalizing the spectra by the number of voxels accounts for these differences.

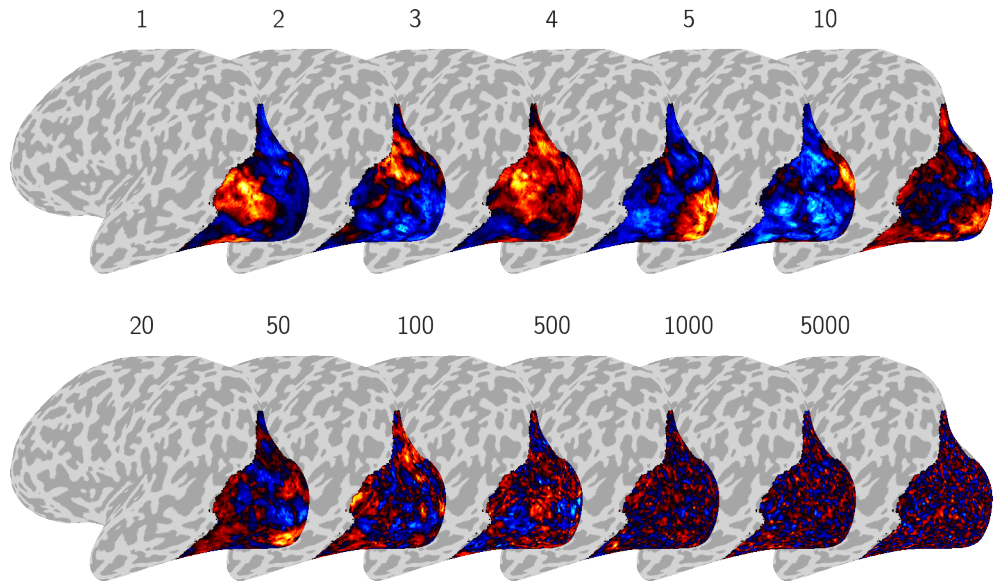


Figure S2: **Examples of singular vectors as a function of rank** obtained from our within-subject cross-decomposition analysis for subject 1 displayed on the cortical surface. The typical spatial scale decreases monotonically with ranks.

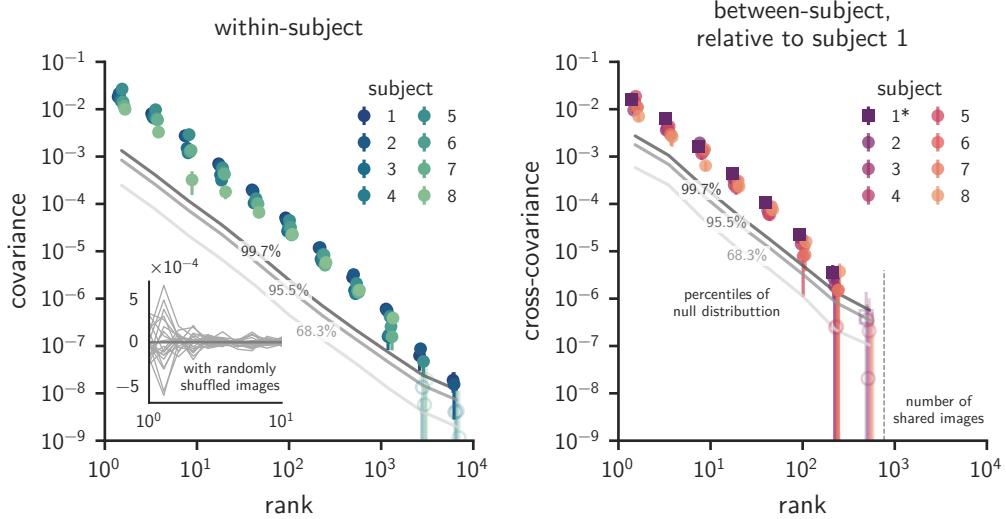


Figure S3: Within- and between-subject covariance spectra compared to null tests. This plot displays the same results as Figure 2 with gray contours indicating the 68th, 95th and 99th percentiles of null distributions obtained by randomly shuffling images before computing the covariance estimates ($n = 5,000$ permutations). Ten samples of this null distribution are displayed in the inset, illustrating that the spectra have an expected value of zero when no reliable covariance is shared between the two datasets. Open symbols denote points that are not significant at $p < 0.001$. This permutation test shows good agreement with the error bars denoting the standard deviations across 8 different splits of the data.

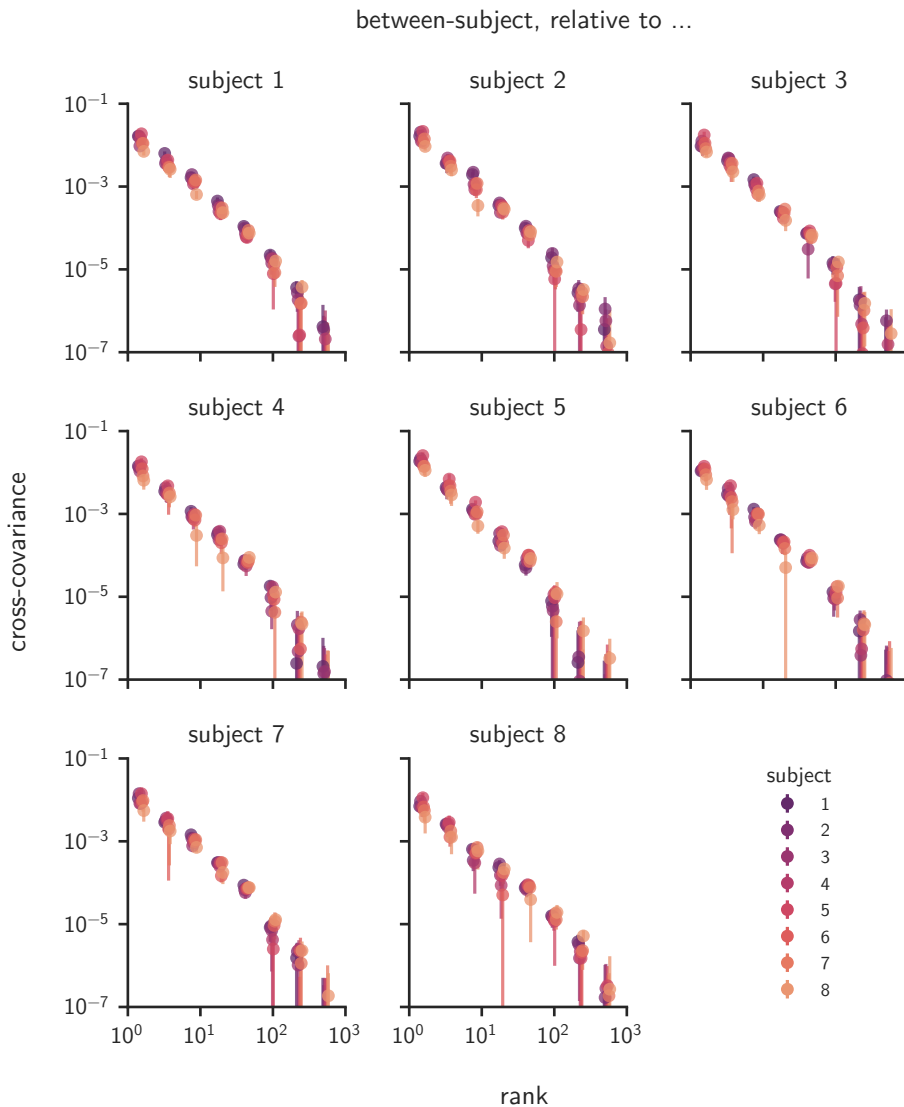


Figure S4: Between-subject covariance spectra in the general visual region, relative to each subject. These plots show the same analysis as in the upper right panel of Figure 2 but with each subject treated as the reference subject.

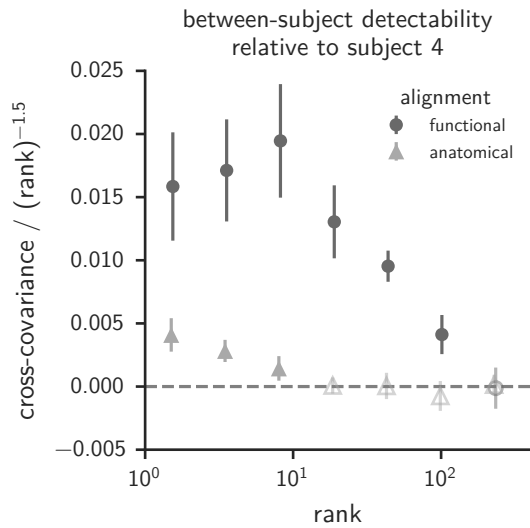


Figure S5: Comparison between cross-spectra obtained using functional and anatomical alignment, relative to a reference subject 1. The two measured spectra are normalized by a power law to visualize their behavior over multiple orders of magnitude. While anatomically alignment reveals only ≈ 10 shared latent dimensions, functionally aligning subjects reveals many more shared latent dimensions. Open symbols denote points where the mean is less than three standard deviations above zero.

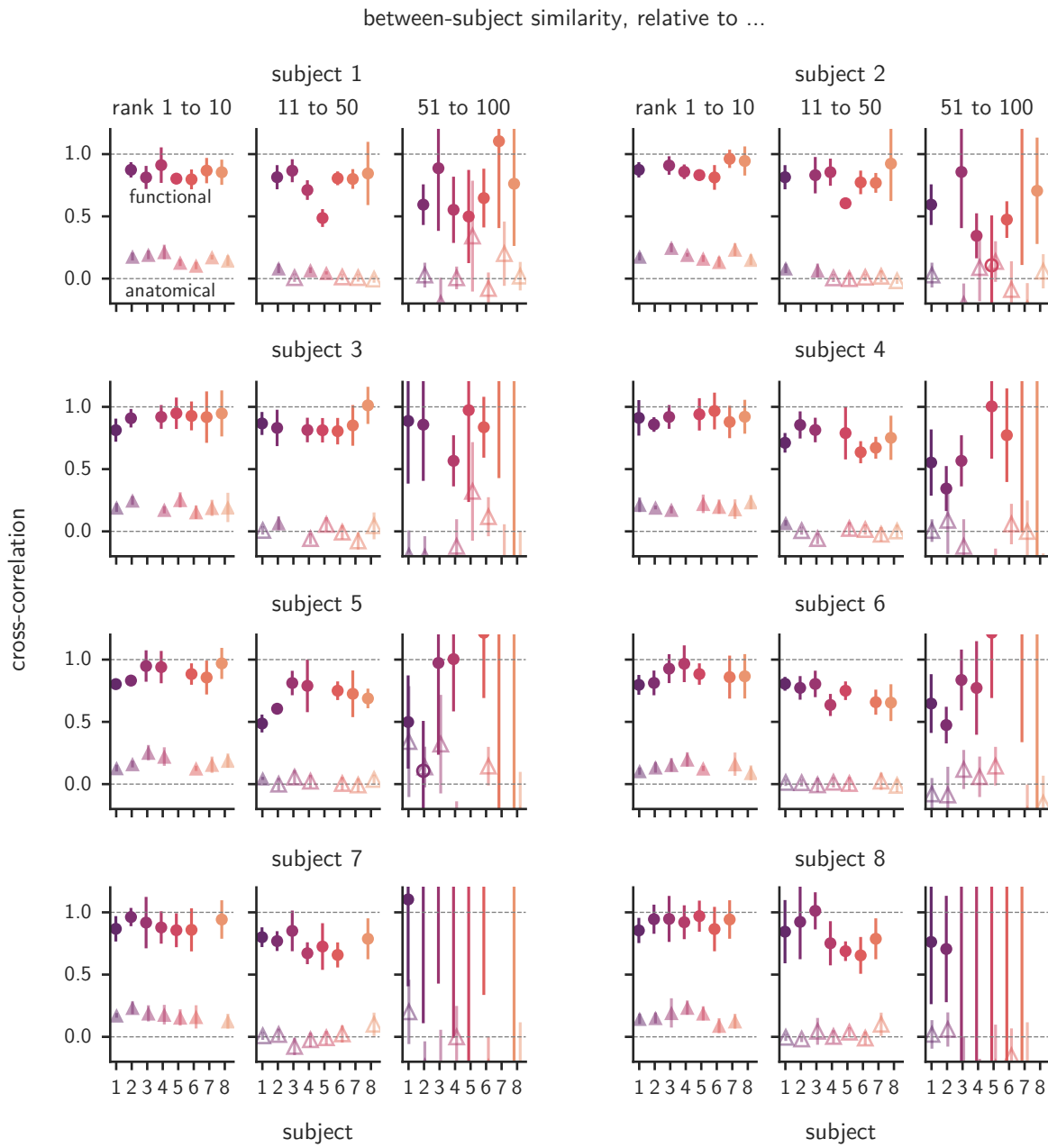


Figure S6: Representational similarity in visual cortex for all pairs of subjects. These plots show the same analysis as in Figure 3 but with each subject treated as the reference subject.

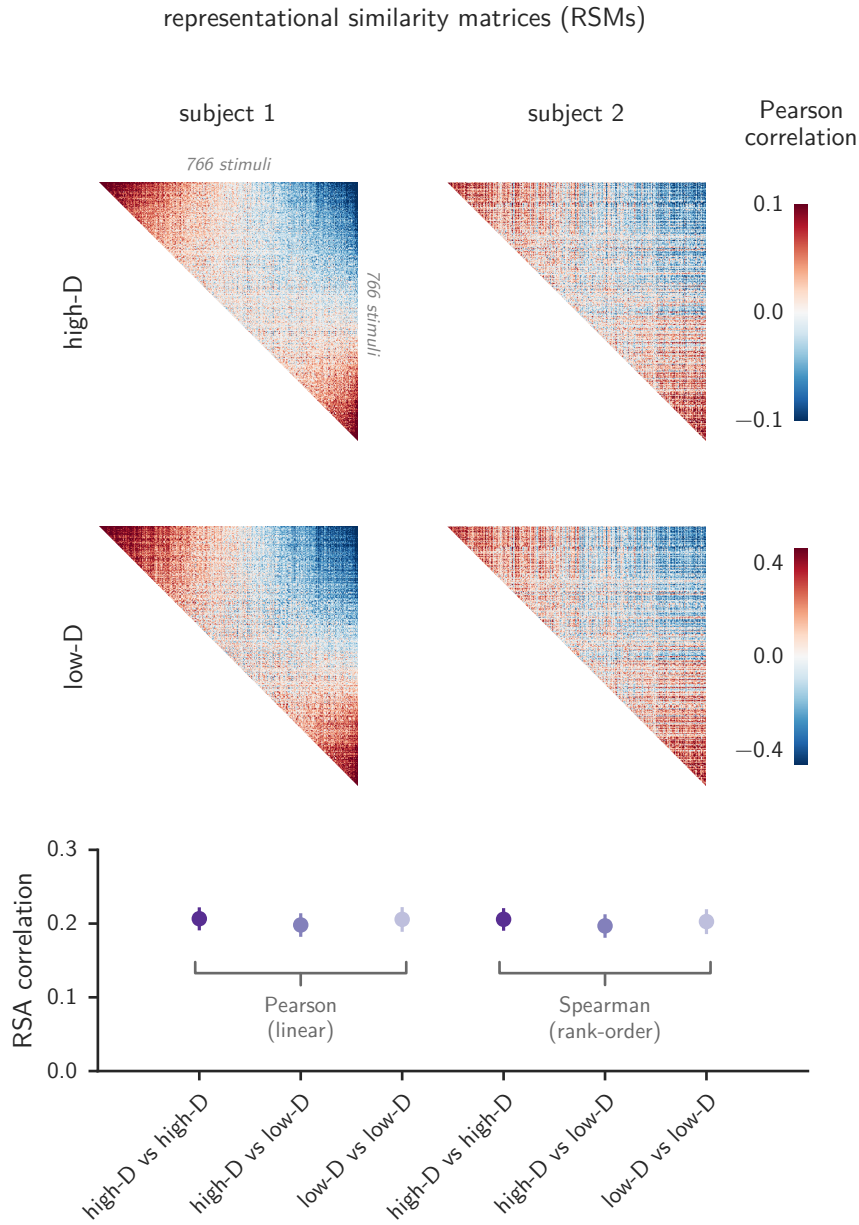


Figure S7: RSA correlations are largely insensitive to high-dimensional structure. Representational similarity analysis (RSA) was used to compare the visual cortex representations of two individuals. (Top) This analysis was performed on two sets of RSMs: one computed on the original fMRI data (“high-D”) and a second computed on reduced-rank fMRI data (“low-D”). Reduced-rank fMRI data was generated by applying principal component analysis to the fMRI response matrices and then reconstructing each matrix from its first 10 principal components (PCs). As can be seen by the RSM visualizations, this dimension-reduction procedure has little effect on the RSMs because the underlying similarity metrics are largely driven by the leading PCs of the response matrices. (Bottom) The mean RSA correlation across all pairs of subjects remains nearly identical even after the data for one subject in each pair has been drastically reduced to just 10 PCs (compare “high-D vs high-D” to “high-D vs low-D”). The same phenomenon is observed when computing RSA scores using both linear Pearson correlations (left) and rank-order Spearman correlations. These results illustrate that variance-weighted similarity metrics, which are dominated by the leading PCs of neural activity, are effectively insensitive to the shared variance at high-rank dimensions that can be detected with our cross-decomposition approach, which extends well beyond 10 ranks (Figure 2). Error bars denote 2 standard deviations across 5,000 bootstrap samples. For each bootstrap sample, 90% of the stimuli were subsampled without repetition before computing representational similarity matrices (RSMs).

References

- Allen, E. J., St-Yves, G., Wu, Y., Breedlove, J. L., Prince, J. S., Dowdle, L. T., Nau, M., Caron, B., Pestilli, F., Charest, I., Hutchinson, J. B., Naselaris, T., & Kay, K. (2021). A massive 7t fMRI dataset to bridge cognitive neuroscience and artificial intelligence. *Nature Neuroscience*, 25(1), 116–126. <https://doi.org/10.1038/s41593-021-00962-x>
- Ansuini, A., Laio, A., Macke, J. H., & Zoccolan, D. (2019). Intrinsic dimension of data representations in deep neural networks. In H. Wallach, H. Larochelle, A. Beygelzimer, F. d'Alché-Buc, E. Fox, & R. Garnett (Eds.), *Advances in neural information processing systems* (Vol. 32). Curran Associates, Inc. https://proceedings.neurips.cc/paper_files/paper/2019/file/cfcce0621b49c983991ead4c3d4d3b6b-Paper.pdf
- Babadi, B., & Sompolinsky, H. (2014). Sparseness and expansion in sensory representations. *Neuron*, 83(5), 1213–1226. <https://doi.org/10.1016/j.neuron.2014.07.035>
- Bao, P., She, L., McGill, M., & Tsao, D. Y. (2020). A map of object space in primate inferotemporal cortex. *Nature*, 583(7814), 103–108. <https://doi.org/10.1038/s41586-020-2350-5>
- Cayco-Gajic, N. A., & Silver, R. A. (2019). Re-evaluating circuit mechanisms underlying pattern separation. *Neuron*, 101(4), 584–602. <https://doi.org/10.1016/j.neuron.2019.01.044>
- Chen, Z., & Bonner, M. F. (2024). Universal dimensions of visual representation. <https://doi.org/10.48550/ARXIV.2408.12804>
- Cohen, U., Chung, S., Lee, D. D., & Sompolinsky, H. (2020). Separability and geometry of object manifolds in deep neural networks. *Nature Communications*, 11(1). <https://doi.org/10.1038/s41467-020-14578-5>
- Connolly, A. C., Guntupalli, J. S., Gors, J., Hanke, M., Halchenko, Y. O., Wu, Y.-C., Abdi, H., & Haxby, J. V. (2012). The representation of biological classes in the human brain. *The Journal of Neuroscience*, 32(8), 2608–2618. <https://doi.org/10.1523/jneurosci.5547-11.2012>
- Contier, O., Baker, C. I., & Hebart, M. N. (2024). Distributed representations of behaviour-derived object dimensions in the human visual system. *Nature Human Behaviour*. <https://doi.org/10.1038/s41562-024-01980-y>
- Cunningham, J. P., & Yu, B. M. (2014). Dimensionality reduction for large-scale neural recordings. *Nature Neuroscience*, 17(11), 1500–1509. <https://doi.org/10.1038/nn.3776>
- De, A., & Chaudhuri, R. (2023). Common population codes produce extremely nonlinear neural manifolds. *Proceedings of the National Academy of Sciences*, 120(39). <https://doi.org/10.1073/pnas.2305853120>
- Elmoznino, E., & Bonner, M. F. (2024). High-performing neural network models of visual cortex benefit from high latent dimensionality (D. Linsley, Ed.). *PLOS Computational Biology*, 20(1), e1011792. <https://doi.org/10.1371/journal.pcbi.1011792>
- Fusi, S., Miller, E. K., & Rigotti, M. (2016). Why neurons mix: High dimensionality for higher cognition. *Current Opinion in Neurobiology*, 37, 66–74. <https://doi.org/10.1016/j.conb.2016.01.010>
- Guth, F., & Ménard, B. (2024). On the universality of neural encodings in CNNs. *ICLR 2024 Workshop on Representational Alignment*. <https://openreview.net/forum?id=ofEBFOrITI>
- Haxby, J. V., Guntupalli, J. S., Connolly, A. C., Halchenko, Y. O., Conroy, B. R., Gobbini, M. I., Hanke, M., & Ramadge, P. J. (2011). A common, high-dimensional model of the representational space in human ventral temporal cortex. *Neuron*, 72(2), 404–416. <https://doi.org/10.1016/j.neuron.2011.08.026>
- Haxby, J. V., Guntupalli, J. S., Nastase, S. A., & Feilong, M. (2020). Hyperalignment: Modeling shared information encoded in idiosyncratic cortical topographies. *eLife*, 9. <https://doi.org/10.7554/elife.56601>
- He, B. J. (2014). Scale-free brain activity: Past, present, and future. *Trends in Cognitive Sciences*, 18(9), 480–487. <https://doi.org/10.1016/j.tics.2014.04.003>
- Hebart, M. N., Contier, O., Teichmann, L., Rockter, A. H., Zheng, C. Y., Kidder, A., Corriveau, A., Vaziri-Pashkam, M., & Baker, C. I. (2023). Things-data, a multimodal collection of large-scale datasets for investigating object representations in human brain and behavior. *eLife*, 12. <https://doi.org/10.7554/elife.82580>
- Huth, A. G., Nishimoto, S., Vu, A. T., & Gallant, J. L. (2012). A continuous semantic space describes the representation of thousands of object and action categories across the human brain. *Neuron*, 76(6), 1210–1224. <https://doi.org/10.1016/j.neuron.2012.10.014>
- Jazayeri, M., & Ostojic, S. (2021). Interpreting neural computations by examining intrinsic and embedding dimensionality of neural activity. *Current Opinion in Neurobiology*, 70, 113–120. <https://doi.org/10.1016/j.conb.2021.08.002>

- Kello, C. T., Brown, G. D., Ferrer-i-Cancho, R., Holden, J. G., Linkenkaer-Hansen, K., Rhodes, T., & Van Orden, G. C. (2010). Scaling laws in cognitive sciences. *Trends in Cognitive Sciences*, 14(5), 223–232. <https://doi.org/10.1016/j.tics.2010.02.005>
- Khosla, M., Ratan Murty, N. A., & Kanwisher, N. (2022). A highly selective response to food in human visual cortex revealed by hypothesis-free voxel decomposition. *Current Biology*, 32(19), 4159–4171.e9. <https://doi.org/10.1016/j.cub.2022.08.009>
- Kornblith, S., Norouzi, M., Lee, H., & Hinton, G. (2019, June). Similarity of neural network representations revisited. In K. Chaudhuri & R. Salakhutdinov (Eds.), *Proceedings of the 36th international conference on machine learning* (pp. 3519–3529, Vol. 97). PMLR. <https://proceedings.mlr.press/v97/kornblith19a.html>
- Kriegeskorte, N. (2008). Representational similarity analysis - connecting the branches of systems neuroscience. *Frontiers in Systems Neuroscience*. <https://doi.org/10.3389/neuro.06.004.2008>
- Kriegeskorte, N., & Diedrichsen, J. (2019). Peeling the onion of brain representations. *Annual Review of Neuroscience*, 42(1), 407–432. <https://doi.org/10.1146/annurev-neuro-080317-061906>
- Lehky, S. R., Kiani, R., Esteky, H., & Tanaka, K. (2014). Dimensionality of object representations in monkey inferotemporal cortex. *Neural Computation*, 26(10), 2135–2162. https://doi.org/10.1162/neco_a_00648
- Lehky, S. R., & Tanaka, K. (2016). Neural representation for object recognition in inferotemporal cortex. *Current Opinion in Neurobiology*, 37, 23–35. <https://doi.org/10.1016/j.conb.2015.12.001>
- Lin, Q., & Newberry, M. (2023). Seeing through noise in power laws. *Journal of The Royal Society Interface*, 20(205). <https://doi.org/10.1098/rsif.2023.0310>
- Lynn, C. W., Holmes, C. M., & Palmer, S. E. (2024). Heavy-tailed neuronal connectivity arises from hebbian self-organization. *Nature Physics*, 20(3), 484–491. <https://doi.org/10.1038/s41567-023-02332-9>
- Manley, J., Lu, S., Barber, K., Demas, J., Kim, H., Meyer, D., Traub, F. M., & Vaziri, A. (2024). Simultaneous, cortex-wide dynamics of up to 1 million neurons reveal unbounded scaling of dimensionality with neuron number. *Neuron*, 112(10), 1694–1709.e5. <https://doi.org/10.1016/j.neuron.2024.02.011>
- Prince, J. S., Fajardo, G., Alvarez, G. A., & Konkle, T. (2024). Manipulating dropout reveals an optimal balance of efficiency and robustness in biological and machine visual systems. *The Twelfth International Conference on Learning Representations*. <https://openreview.net/forum?id=ADDCErFzev>
- Roads, B. D., & Love, B. C. (2024). The dimensions of dimensionality. *Trends in Cognitive Sciences*. <https://doi.org/10.1016/j.tics.2024.07.005>
- Stringer, C., Pachitariu, M., Steinmetz, N., Carandini, M., & Harris, K. D. (2019). High-dimensional geometry of population responses in visual cortex. *Nature*, 571(7765), 361–365. <https://doi.org/10.1038/s41586-019-1346-5>
- Tarhan, L., & Konkle, T. (2020). Sociality and interaction envelope organize visual action representations. *Nature Communications*, 11(1). <https://doi.org/10.1038/s41467-020-16846-w>
- Thorat, S., Proklova, D., & Peelen, M. V. (2019). The nature of the animacy organization in human ventral temporal cortex. *eLife*, 8. <https://doi.org/10.7554/elife.47142>